

Title	High field effect on ultrafast pump-probe excitation of compound semiconductors
Author(s)	Iida, Masaru; Katayama, Shin'ichi
Citation	Physica B : Condensed Matter, 314(1-4): 288-292
Issue Date	2002-03
Type	Journal Article
Text version	author
URL	http://hdl.handle.net/10119/4971
Rights	<p>NOTICE: This is the author 's version of a work accepted for publication by Elsevier. Changes resulting from the publishing process, including peer review, editing, corrections, structural formatting and other quality control mechanisms, may not be reflected in this document. Changes may have been made to this work since it was submitted for publication.</p> <p>A definitive version was subsequently published in Masaru Iida and Shin'ichi Katayama, Physica B : Condensed Matter, 314(1-4), 2002, 288-292, http://dx.doi.org/10.1016/S0921-4526(01)01422-3</p>
Description	

High field effect on ultrafast pump-probe excitation of compound semiconductors

^a Masaru Iida and ^b Shin'ichi Katayama

^a *Kansai Advanced Research Center, Communications Research Laboratory 588-2, Iwaoka, Nishi-ku, Kobe, Hyogo 651-2492, Japan*

^b *School of Materials Science, Japan Advanced Institute of Science and Technology, 1-1 Asahidai, Tatsunokuchi, Ishikawa 923-1292, Japan*

e-mail: miida@crl.go.jp, TEL: 81+78-969-2198, FAX: 81+78-969-2219

Abstract

The pump-probe excitation of compound semiconductors in the presence of high electric fields is studied with a model of non-interacting photo-excited electron-hole system theoretically. Coherent excitation of the interband polarization produces an oscillatory structure in the carrier density and the differential transmission spectrum (DTS) above the band gap. The DTS profile is altered by the effect of a high electric field on both the pump excitation and the probe excitation. Our analysis reveals that the pump excitation with relatively longer pulse (100 fs) induces the oscillatory structure in the DTS while the probe excitation with short pulse (20 fs) gives rise to a peak shift towards the lower energy side due to the field assisted generation. The oscillation period in the DTS depends on the electric field to the two-third power, which corresponds to the Franz-Keldysh oscillation.

Key words: ultrafast kinetics, high electric field, pump-probe method

PACS: 78.47.+p

1. Introduction

Recent progress on the ultrashort pulse laser technology has enabled us to observe carrier dynamics in a real-time region. In particular, the pump-probe technique gives us a lot of insight into the ultrashort phenomena related to the carrier dynamics in semiconductors. Several experimental studies on ultrafast carrier dynamics under the influence of a high electric field were reported recently [1,2]. Herbst et al. [3] carried out a theoretical study of the ultrafast behavior of carriers in a quantum wire, in the presence of an electric field. We have recently reported the evolution of carrier density matrices in an ultrashort time in the presence of high electric fields by taking into account carrier-longitudinal optical(LO) phonon scattering[4,5]. However, it is still not clear how does the high electric effect appear in the experiments such as a differential transmission spectrum (DTS) measurement. In the present study, we explore the pump-probe excitation of a compound semiconductor in the presence of a high electric field theoretically. To simplify our analysis, we neglect carrier-carrier and carrier-LO phonon interactions. We find that oscillatory structures appear in both the carrier density distribution and the DTS. It is shown that a peak shift due to the field-assisted generation [3] and the formation of an oscillatory structure are seen in the carrier density distribution, while the oscillatory structure is observed clearly in the DTS with the peak shift due to the field assisted generation. These oscillatory structures are similar with the Franz-Keldysh oscillation.

2. Excitation in high electric field

For simplicity, a direct gap semiconductor, such as GaAs, in an electric field E along the z -axis was being considered. To focus on the high electric field effect on the excitation process, we ignored any carrier scattering mechanisms. Thus, our Hamiltonian reads $H = H_0 + H_L$, where H_0 and H_L denote free carrier part and and classical light-carrier interaction. In the representation of the second quantization, the non-interacting part is given by $H_0 = \sum_{\mathbf{k}\nu} \epsilon_{\mathbf{k}\nu}^e c_{\mathbf{k}\nu}^\dagger c_{\mathbf{k}\nu} + \sum_{\mathbf{k}\lambda} \epsilon_{\mathbf{k}\lambda}^h d_{\mathbf{k}\lambda}^\dagger d_{\mathbf{k}\lambda}$. The operators $c^\dagger(d^\dagger)$ and $c(d)$ denote the electron (hole) creation and annihilation operators, respectively, and $\mathbf{k} = (k_x, k_y)$. The single-particle energy of an electron and a hole can be written as $\epsilon_{\mathbf{k}\nu}^e = \nu\epsilon_0 + \hbar^2\mathbf{k}^2/2m_e^* + E_g$ and $\epsilon_{\mathbf{k}\lambda}^h = \lambda\epsilon_0 + \hbar^2\mathbf{k}^2/2m_h^*$, where E_g is the band gap energy, $m_{e(h)}^*$ is the electron (hole) effective mass, and $\epsilon_0 = (\hbar^2 F^2/2m_r)^{1/3}$ is the so-called electro-optical energy. Here, m_r denotes the reduced mass $m_r = m_e^*m_h^*/(m_e^*+m_h^*)$ and $F = eE$, with the charge e . The corresponding electron envelope function [5–7] is $\psi_{\mathbf{k}\nu}^e(\mathbf{x}_\perp, z) = \sqrt{\frac{2\epsilon_0}{FS}} e^{i\mathbf{k}\cdot\mathbf{x}_\perp} \left(\frac{2m_r^*F}{\hbar^2}\right)^{\frac{1}{3}} \zeta_\nu(z)$,

where $\zeta_\nu(z) \equiv \text{Ai} \left[-\left(\frac{2m_e^* F}{\hbar^2}\right)^{\frac{1}{3}} \left(z + \frac{\nu \epsilon_0}{F}\right) \right]$ and $\mathbf{x}_\perp = (x, y)$, S being the normalization area. Using this formula, we obtained the light-carrier interaction in high electric fields as

$H_L = \sum_{\mathbf{k}\nu\lambda} \left\{ d^{eh} \chi_{\nu,-\lambda}^{eh} E_L(t) c_{\mathbf{k}\nu}^\dagger d_{-\mathbf{k}-\lambda}^\dagger + d^{he} \chi_{-\lambda,\nu}^{he} E_L^*(t) d_{-\mathbf{k}-\lambda} c_{\mathbf{k}\nu} \right\}$. In H_L , we used the overlap integral [7] $\chi_{\nu,\lambda}^{eh} = 2\sqrt{\pi} \text{Ai}(\nu + \lambda)$. Through the overlap integral, the states along the electric field direction are coupled each other when the light pulse enters the sample. We can obtain physical quantities using the density matrices (DMs) $n_{\mathbf{k},\nu,\lambda}^e = \langle c_{\mathbf{k}\nu}^\dagger c_{\mathbf{k}\lambda} \rangle$ for an electron, and $n_{-\mathbf{k},-\nu,-\lambda}^h = \langle d_{-\mathbf{k}-\nu}^\dagger d_{-\mathbf{k}-\lambda} \rangle$ for a hole and the interband polarization $p_{\mathbf{k},-\nu,\lambda} = \langle d_{-\mathbf{k}-\nu} c_{\mathbf{k}\lambda} \rangle$. The equations of motion for these DMs are defined using $\frac{\partial}{\partial t} n_{\mathbf{k},\nu,\lambda}^e = \frac{i}{\hbar} \langle [H, c_{\mathbf{k}\nu}^\dagger c_{\mathbf{k}\lambda}] \rangle$ in the Heisenberg picture. These coupled equations can be written as

$$\begin{aligned} \frac{\partial n_{\mathbf{k},\nu,\lambda}^e}{\partial t} &= \frac{i}{\hbar} (\nu - \lambda) \epsilon_0 n_{\mathbf{k},\nu,\lambda}^e \\ &- \frac{i}{\hbar} \sum_{\mu} \left\{ d^{eh} \chi_{\lambda,-\mu}^{eh} E(t) p_{\mathbf{k}-\mu,\nu}^* - d^{he} \chi_{-\mu,\nu}^{he} E^*(t) p_{\mathbf{k}-\mu,\lambda} \right\} \end{aligned} \quad (1)$$

for an electron, and a similar one can be obtained for a hole. For the interband polarization, we have

$$\begin{aligned} \frac{\partial p_{\mathbf{k}-\nu,\lambda}}{\partial t} &= -\frac{i}{\hbar} (\epsilon_{\mathbf{k}\lambda}^e + \epsilon_{-\mathbf{k}-\nu}^h) p_{\mathbf{k}-\nu,\lambda} \\ &+ \frac{i}{\hbar} \sum_{\mu} \left\{ d^{eh} \chi_{\mu,-\nu}^{eh} E(t) n_{\mathbf{k}\mu,\lambda}^e - d^{eh} \chi_{\mu,-\lambda}^{eh} E(t) (1 - n_{-\mathbf{k}-\mu,\lambda}^h) \right\}. \end{aligned} \quad (2)$$

3. Numerical Analysis and Results

We solved the equations of motion numerically and obtained DTS using the following method. The material parameters of GaAs were assumed to be $m_e^* = 0.063m_0$, $m_h^* = 0.45m_0$ and $E_g = 1.45$ eV. Since we have ignored the carrier scattering, we can solve the equations of motion for each \mathbf{k} independently. This calculation can be transformed into the energy space from the \mathbf{k} -space. We simulated the pump-probe experiment using separate calculations of “pump-on” and “pump-off” cases. The transmission spectrum $T(\omega)$ is proportional to the imaginary part of the interband polarization $P(\omega)$ [8]. Thus the DTS can be calculated with the following formula [9],

$$DTS(\omega) = \frac{T_p(\omega) - T_0(\omega)}{T_0(\omega)} \propto -\frac{\text{Im}[P_p(\omega) - P_0(\omega)]}{E_0(\omega)}, \quad (3)$$

where $T_p(P_p)$ corresponds to “pump-on” signal, $T_0(P_0)$ is “pump-off” transmitted one, and E_0 is laser electric field of the probe pulse. Since even the calculation the time evolution of DMs in a high electric field requires huge computational resources, it is difficult to compute their Fourier transform completely. Thus, we adopt following approximation. Using the Gaussian pulse with a duration τ_L as $E_i(t) = E_i e^{-i\omega_L t} e^{-(t/\tau_L)^2}$, we can formally integrate Eq.(2) assuming appropriate initial distribution. The solution can be written as $p_{k\nu\lambda}(t) = f(k, \nu, \lambda; t) e^{-i(\epsilon_{k\lambda}^e + \epsilon_{-k-\nu}^h - \hbar\omega_L)t}$. The Fourier transform of this integral form introduces $\delta(\epsilon_{k\lambda}^e + \epsilon_{-k-\nu}^h - \hbar\omega_L)$ to the $p_{k\nu\lambda}(\omega)$, because the pulse envelope has longer time scale than the oscillation period of the excitation laser. This is true for the present case. So, the plot of $\sum_{\nu,\lambda} p_{k\nu\lambda}$ as a function of $(\epsilon_k^e + \epsilon_{-k}^h)$ can approximate the spectrum of $P_{p(0)}(\omega) = \int_{-\infty}^{\infty} \sum_k \sum_{\nu,\lambda} p_{k\nu\lambda}(t) e^{-i\omega t} dt$. Using this approximation, we calculated the DTS by changing the time delay, δt , between the pump and probe pulse. The laser electric field can be written as

$$E_i(t) = (1/2) \left\{ E_i^{\text{pump}} e^{-i\omega_L^{\text{pump}} t} e^{-((t-\delta t)/\tau_L^{\text{pump}})^2} + E_i^{\text{probe}} e^{-i\omega_L^{\text{probe}} t} e^{-(t/\tau_L^{\text{probe}})^2} + c.c. \right\}.$$

We started our calculations from $-5 \tau_L^{\text{probe}}$ and ended them after enough long time at which the pump and the probe pulses had gone.

Before our investigation of the DTS, we briefly discuss the interband electron DMs in the presence of a high electric field. Fig. 1 shows the temporal evolution of the electron distribution function $n_{k00}^e(t)$ in the (t, ϵ_k^e) plane assuming $\tau_L = 100$ fs, the detuning energy, $\hbar\omega_L - E_g = 120$ meV and $E = 100$ kV/cm. An obvious oscillatory structure is seen in the electron density as a function of energy. It was suggested numerically for the quantum wires that the main peak would be shifted towards a lower energy side due to the field assisted generation of carriers [3]. In the present treatment based on the Airy function description, we can see the peak shift of the distribution function. More detailed analysis of carrier DMs will be explored elsewhere.

To simulate the DTS based on the approximation described above, we used 100 fs Gaussian pulse as a pump beam and a 20 fs Gaussian pulse as a probe beam. In the present calculations of DTS, the ratio $E_i^{\text{pump}} : E_i^{\text{probe}} = 5 : 1$ is assumed and the detuning of the pump and the probe pulses are assumed to be 120 meV. Fig. 2 shows the DTS as function of energy for $\delta t = -50, 0$ and 100 fs in a static electric field of 100 kV/cm. We found a similar oscillatory behavior in the DTS with that of electron DMs. The amplitude of oscillation increases as δt changes from negative to

positive. The origin of the oscillation can be attribute to the interference among the states in the direction of a static electric field. It is also evident that the spectrum for the negative delay has an opposite phase compared with that for the positive delay. This oscillation is different from those appear in the absence of electric field for negative delay [9].

Fig. 3 shows the dependence on the electric field strength of the DTS for $\delta t = 100$ fs. The static electric fields were assumed to be 25, 50 and 100 kV/cm. In the vicinity of the energy band gap (~ 1.45 eV) the DTS exhibits a quite large amplitude of the oscillation while each DTS shows oscillation as a function of energy with the proper period and decay in the higher energy region. The oscillation takes place through $\text{Ai} \left[(\epsilon_{k\lambda}^e + \epsilon_{-k-\nu}^h - \hbar\omega_L) / \epsilon_0 \right]$ whose period is proportional to the two-third power of electric field.

To analyze the details of the DTS, we depicted the imaginary part of $P_i(\omega)$ (the suffix i denotes pump-on(=p) or pump-off(=0)) and $E_0(\omega)$ for $\delta t = 100$ fs under 25, 50 and 100 kV/cm. These quantities construct the DTS (see Eq. (3)). From Fig. 4(a) and 4(b), the oscillatory structure is assigned clearly as the result of the pump excitation. As is shown in Fig 4(b), the broadened band and the peak shift towards lower energy side in proportional to the increase of E in $\text{Im}P_0$ are attributed to the energy uncertainty due to very short probe pulses and the increment of the field assisted generation. This lead us a conjecture that the DTS would exhibit the clear peak shift due to the field assisted generation if the shorter pump pulse was used.

In summary, the present work simulated numerically the pump-probe excitation of compound semiconductor with a model of non-interacting photo-excited electron-hole system. We emphasized the appearance of oscillatory behavior in the DTS above the band gap energy in the presence of high electric fields. Since it is known that the Coulomb interaction between photo-excited electron and hole plays a important role in the DTS, we will develop the simulation taking into account the Coulomb interaction. The actual experimental conditions such as the scattering of pumped photons, which is not taken in the present work, should be also considered in our future study.

References

- [1] W. Sha et al., Phys. Rev. Lett. **67**, 2553 (1991).
- [2] A. Leitenstorfer et al., Phys. Rev. Lett. **82**, 5140 (1999).
- [3] M. Herbst et al., Phys. Stat. Sol.(b)**204**, 358 (1997).
- [4] M. Iida and S. Katayama, Physica B **272**, 344 (1999).
- [5] M. Iida and S. Katayama, Solid State Commun. **67**, 2553 (2001).
- [6] R. Bertoncini et al., Phys. Rev. B **41**, 1390 (1990).
- [7] A. V. Kuznetsov and C. J. Stanton, Phys. Rev. B **48**, 10828 (1993).
- [8] C. Fürst et al., Phys. Rev. Lett. **78**, 3733 (1997).
- [9] H. Haug and S. W. Koch, Quantum Theory of the Optical and Electronic Properties of Semiconductors 3rd Ed., (World Scientific, Singapore, 1994, and K. El Sayed and C. J. Stanton, Phys. Rev. B **55**, 9671 (1997).

Fig. 1. Electron density distribution versus time and energy in the electric field of 100 kV/cm.

Fig. 2. Differential transmission spectra for $\delta t = -50, 0$ and 100 fs. The static electric field was assumed to be 100 kV/cm.

Fig. 3. Differential transmission spectra for $\delta t = 100$ fs. Static electric fields were assumed to be 25, 50 and 100 kV/cm.

Fig. 4. $-\text{Im}(P_p - P_0)$, E_0 (a) and $\text{Im}P_0$ (b) for $\delta t = 100$ fs in the electric fields of 25, 50 and 100 kV/cm.

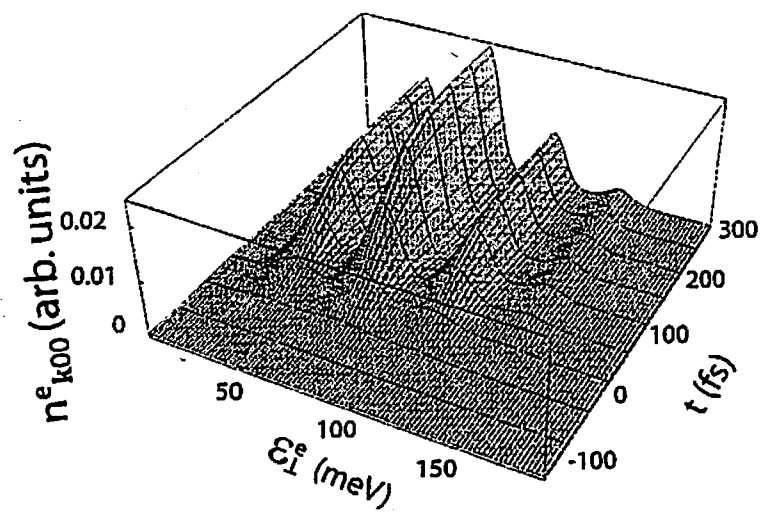


Fig. 1

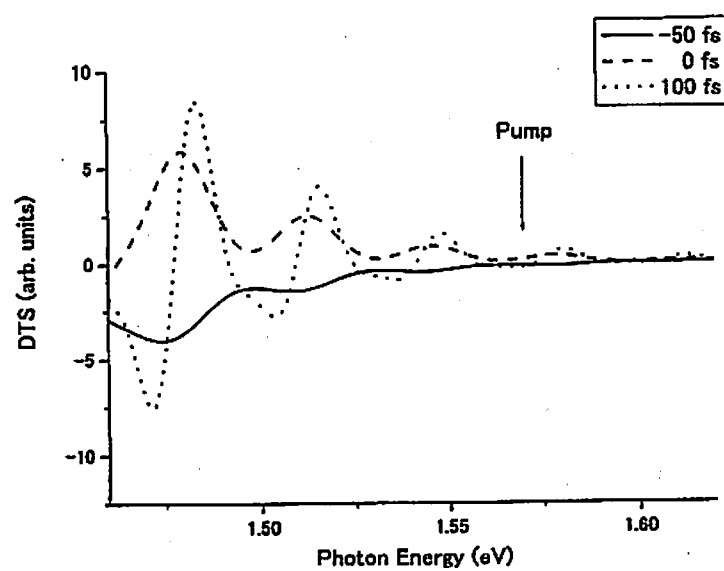


Fig. 2

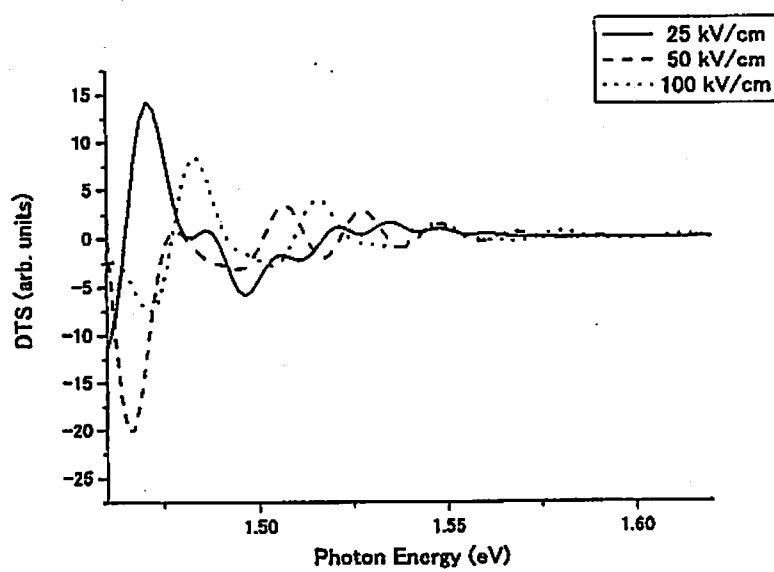


Fig. 3

1.45
0.2
1.57